Geoacoustic inversion in time domain using ship of opportunity noise recorded on a horizontal towed array

Cheolsoo Park
Korea Ocean Research & Development Institute/Korea Research Institute of Ships & Ocean Engineering, 171 Jang-Dong Yuseong, Daejon, Korea

Woojae Seong
Department of Naval Architecture and Ocean Engineering, Seoul National University, Seoul 151-744, Korea

Peter Gerstoft
Marine Physical Laboratory, Scripps Institute of Oceanography, University of California, La Jolla, California 92093

(Received 6 September 2004; revised 6 January 2005; accepted 8 January 2005)

A time domain geoacoustic inversion method using ship noise received on a towed horizontal array is presented. The received signal, containing ship noise as a source of opportunity, is time-reversed and then back-propagated to the vicinity of the ship. The back-propagated signal is correlated with the modeled signal which is expected to peak at the ship's location in case of a good match for the environment. This match is utilized for the geoacoustic parameter inversion. The objective function for this optimization problem is thus defined as the normalized power focused in an area around the source position, using a matched impulse response filter. A hybrid use of global and local search algorithms, i.e., GA and Powell's method is applied to the optimization problem. Applications of the proposed inversion method to MAPEX 2000 noise experiment conducted north of the island of Elba show promising results, and it is shown that the time domain inversion takes advantage of dominant frequencies of the source signature automatically. © *2005 Acoustical Society of America.*
[DOI: 10.1121/1.1862574]

PACS numbers: 43.30.Pc [AIT] Pages: 1933–1941

I. INTRODUCTION

Nowadays the use of passive sonar systems to acquire the information of sources, especially in shallow water areas, is increasing. In addition, various numerical models have been used to simulate their performances with measured or estimated environments, among which the seabed properties are considered to be one of the most influential parameters on the shallow water sound propagation. Therefore, various techniques to estimate the geoacoustic parameters of the ocean bottom via remote sensing have been developed in order to resolve the problem of high cost and time consumption in relation to direct measurement of the sub-bottom properties.

Most areas of the ocean, especially in shallow waters, show varying seabed characteristics that require range-dependent parametrizations for geoacoustic inversion. However, a full range-dependent inversion that can identify the ocean bottom structure simultaneously has not yet been achieved due to computational burdens in forward modeling. A majority of the inversions in underwater acoustics have been performed with the assumption of range-independent environments using long-range propagation data received on a vertical line array (VLA) that produces spatially averaged output.[1,2] In order to avoid this degradation of resolution, towed horizontal line array (HLA) inversion schemes have been proposed and implemented.[3–6] The short distance between a sound source and HLA enables us to simplify the range dependence into local segments of range-independent sectors.[6] The towed HLA system possesses additional advantages of mobility and manageability, which are inherently suitable for a towed sonar system compared to a VLA.

Inversions which utilize the full structure of the bottom reflected signals usually require well controlled acoustic sources. Such dedicated sources may add extra burdens to an inversion experiment especially of the towed HLA system. Contrary to controlled sources, the noise of the tow ship or ship of opportunity can be a good alternative source for inversion.[5,7] Most of the analyses with the acquired data are processed in the frequency domain, both at the narrowband and broadband, with the exception of a few that have been chosen to deal directly in the time domain.[6,8–13] Since the ship noise shows a broadband characteristic, it is needed to extract strong tonal components in frequency domain inversions.[5] On the contrary, time domain inversions can take advantage of a full broadband signal without having to go through the necessary processing.

The inversion is usually formulated as an optimization problem enabling various optimization techniques to be applied to the inverse problems, such as a global optimization[14,15] and a hybrid form of global and local search.[16,17] The solutions of the optimization can be regarded as the parameters which optimize the objective function defined to measure the difference (or similarity) between received and simulated data. Although it is common for all parameters to be inverted simultaneously, iterative optimizations can be performed after grouping the parameters based on their sensitivities.[18]

In this paper, a time domain inversion using ship noise

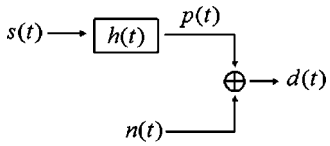

FIG. 1. An idealized data acquisition system where the received signal $d(t)$ is comprised of the propagated signal $p(t)$ and noise $n(t)$.

acquired on a towed HLA is proposed. An objective function is defined using a matched impulse response filter for the unknown source signal and the filtered output is implemented by back-propagating the time-reversed signal using a ray-based model. Then, a series of global and local searches is applied to measured data in order to find the optimum parameters of the inverse problem.

The paper is organized as follows. In Sec. II we describe a matched impulse response filter which is a basic theory used in defining the objective function. In Sec. III, a sensitivity test is also presented related to the objective function. In Sec. IV we describe the MAPEX 2000 noise experiment and the parametrization of the inversion. In Sec. V we present the geoacoustic inversion results using the source of opportunity.

II. MATCHED IMPULSE RESPONSE FILTER

It has been demonstrated that the sound wave received by a hydrophone and retransmitted backwards focuses at the source position.[19] This phenomenon can be implemented numerically using a received signal as a virtual source, which was utilized in source localization.[20,21] It has also been used in underwater applications such as pulse compressing for the communications in the name of time reversal or phase conjugation.[22,23] The wave focusing is explained via matched filtering and array processing.

A data acquisition process can be represented by an idealized system of Fig. 1, where the received signal $d(t)$ is comprised of propagated signal $p(t)$ and noise $n(t)$. In the linear time invariant system, the propagation of source signal $s(t)$ through a medium can be simply expressed by convolution with an impulse response $h(t)$ as

$$d(t)=p(t)+n(t)=s(t)*h(t)+n(t). \tag{1}$$

The rigorous impulse response for wave propagating in the ocean can be found by solving the wave equation. However, for a set of source and receiver separated within a few water depths, the received signal can be approximated by the sum of eigen-rays weighted and delayed according to their propagation paths. Thus, ignoring the noise for the moment, the received signal can be expressed as

$$d(t)=s(t)*h(t)=s(t)*\sum_{i=1}^{M} a_i\delta(t-\tau_i), \tag{2}$$

where a_i and τ_i represent the amplitude decay and travel time of the signal component which are propagated through M different paths (eigen-rays), respectively.

If this signal is time reversed and back-propagated, then the medium impulse response simply becomes $h(-t)$, called

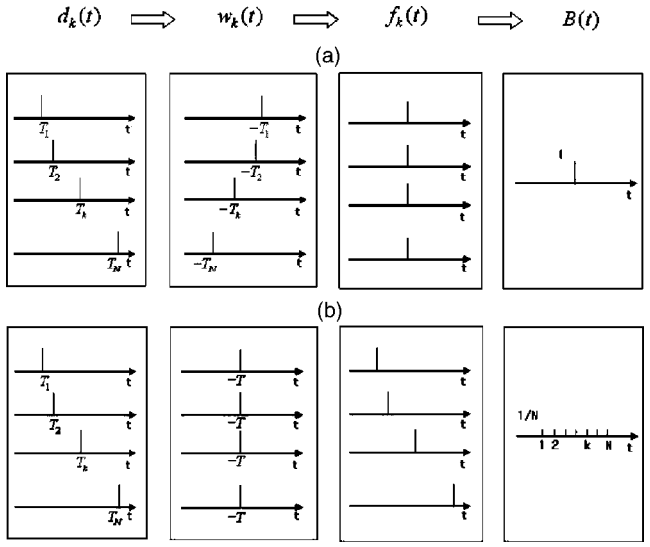

FIG. 2. Examples of beamforming using an impulse signal; (a) optimally beamformed signal and (b) nonoptimally beamformed signal.

the matched impulse response. Applying this as a filter $w(t)$ produces an output at the source location given by

$$\begin{aligned} f(t)&=d(t)*h(-t)\\ &=\sum_{i=1}^{M} a_i^2 s(t)+\sum_{i=1}^{M}\sum_{j\neq i}^{M} a_i a_j s(t-(\tau_i-\tau_j)). \end{aligned} \tag{3}$$

It can be seen from Eq. (3) that the filter output comprises of two components, $\Sigma_{i=1}^{M} a_i^2 s(t)$ and $\Sigma_{i=1}^{M}\Sigma_{j\neq i}^{M} a_i a_j s(t-(\tau_i-\tau_j))$, which correspond to a mainlobe and multiple sidelobes of the signal, respectively.

Now, the plane-wave beam-forming concept can be extended for an array with N receivers such that the back-propagated output power is defined as

$$\begin{aligned} B(t)&=\frac{1}{N}\sum_{k=1}^{N} f_k(t)\\ &=\frac{1}{N}\sum_{k=1}^{N}\sum_{i=1}^{M} a_{i,k}^2 s(t)\\ &\quad+\frac{1}{N}\sum_{k=1}^{N}\sum_{i=1}^{M}\sum_{j\neq i}^{M} a_{i,k}a_{j,k}s(t-(\tau_{i,k}-\tau_{j,k})). \end{aligned} \tag{4}$$

If the filter is correct, the mainlobe will be reinforced whereas the sidelobes are cancelled by destructive interference. As a result, the mainlobe becomes dominant over the sidelobes as the number of channels increase [Fig. 2(a)]. If the filter is presumed incorrectly, which corresponds to an environmental mismatch, there will be multiple mainlobes along with additional sidelobes [Fig. 2(b)].

The ocean environment itself can be considered as a filter when the received signal is retransmitted reversely. Therefore, when the environment and also the source receiver configurations are modeled as when the signal was recorded at the receiver array, the retransmitted signal will be focused at the original source position.

III. GEOACOUSTIC INVERSION USING SHIP NOISE

Acoustic signals transmitted by a source convey information of the medium through which they propagated. There are numerous acoustic sources for ocean experiments, and the noise generated by a ship is one which will be present most of the time when experiments are carried out in the ocean. If the waveform of a ship noise is unknown, only the impulse response can be used in the geoacoustic inversion.

Inversion parameters which describe the environment are represented by a model vector $\overline{\mathbf{m}}=[\overline{m}_1,\overline{m}_2,\ldots,\overline{m}_L]^T$, where $[\ ]^T$ is a transpose operator. The normalized filter output of the channel is defined as

$$f_k(t,\overline{\mathbf{m}})=\frac{d_k(T-t)}{\sqrt{\int_{-\infty}^{\infty}|d_k(T-t)|^2dt}}*\frac{\overline{h}_k(t,\overline{\mathbf{m}})}{\sqrt{\int_{-\infty}^{\infty}|\overline{h}_k(t,\overline{\mathbf{m}})|^2dt}}, \tag{5}$$

where $\overline{h}_k(t,\overline{\mathbf{m}})$ is an impulse response of the corresponding environment. Equation (5) is implemented by propagating the received and time-reversed signal through the environment using a forward model. The objective function to be maximized for the inversion using N receivers is defined as

$$\phi(\overline{\mathbf{m}})=\max\left(\frac{1}{\Delta T}\int_{T_1}^{T_1+\Delta T}|B(t,\overline{\mathbf{m}})|^2dt\right),\quad 0\leqslant T_1\leqslant T-\Delta T, \tag{6}$$

where

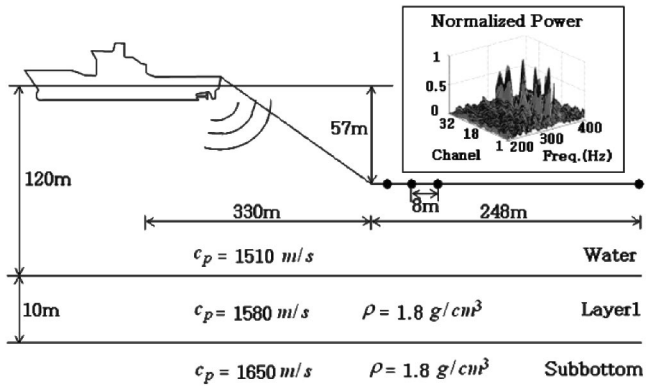

FIG. 3. The shallow water environment and the geometry of towed array system used for the sensitivity test. The power spectrums of measured signals which are simulated based on the given environment are also shown in the figure.

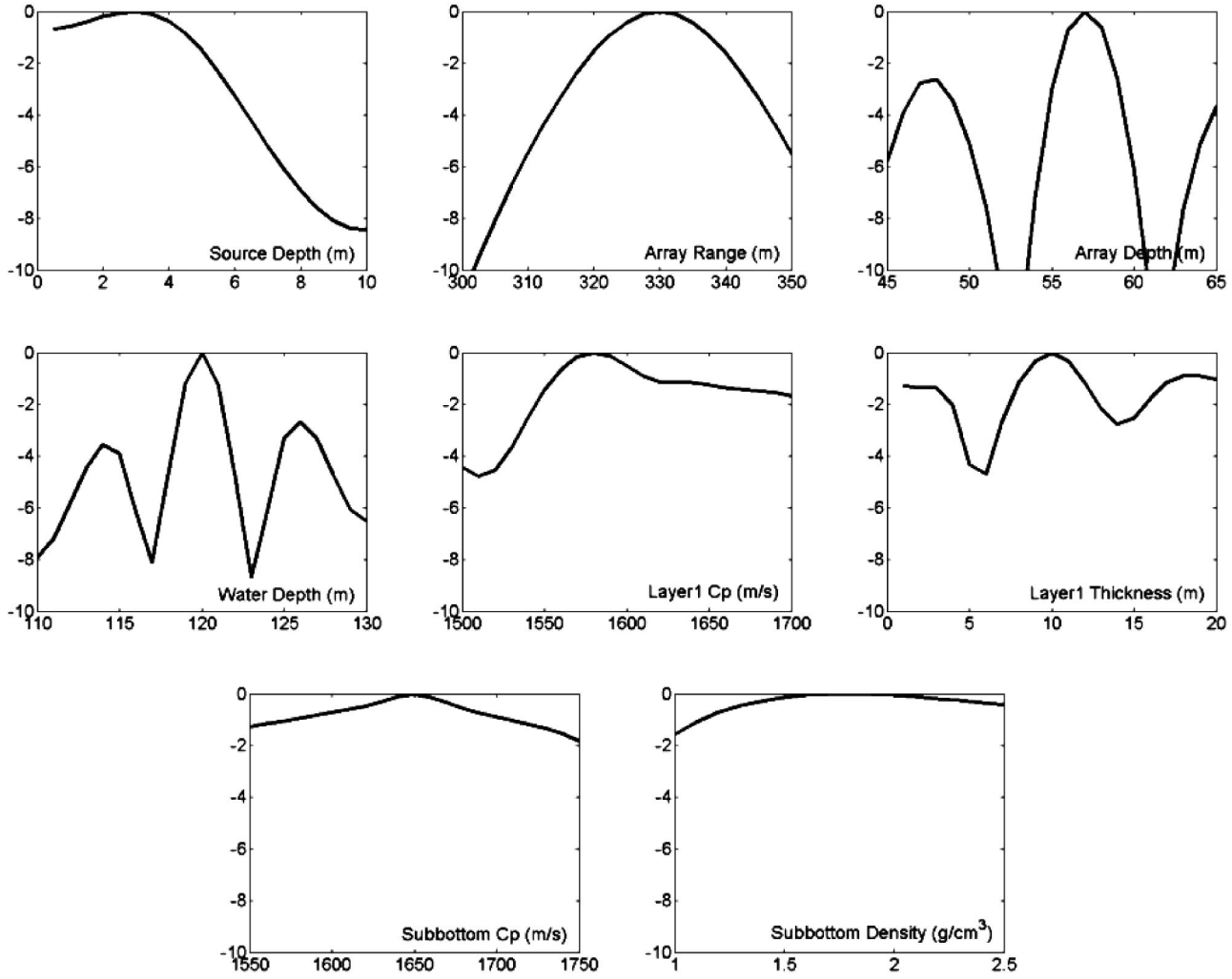

FIG. 4. Sensitivity curves of various parameters which show the objective function values evaluated at the parameter values given in the x-axis. Meanwhile, other parameters are fixed at their reference values given in Fig. 3. Note that the function values are given in dB normalized to the maximum value.

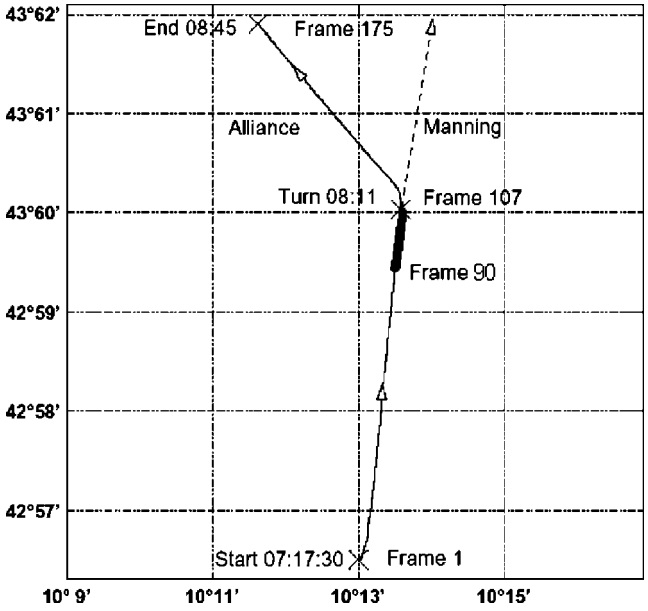

FIG. 5. The tracks of the RV *Alliance* and *Manning* during the experiment. The thick line indicates the track of *Manning* used as sources of opportunity in geoacoustic inversions.

$$B(t,\overline{\mathbf{m}}) = \frac{1}{N}\sum_{i=1}^{N} f_i(t,\overline{\mathbf{m}}). \tag{7}$$

A ray-based model is chosen for the forward model to calculate the objective function. In order to construct the impulse response in the ray-based model, we need information of amplitudes and phases of the rays that arrive at the receiver position within a predetermined error bound.[6] It was found that a simple plane wave approximation is sufficient to calculate the phase and amplitude of a ray if the grazing angel of the ray is not near the critical angle, which corresponds to our inversion case presented in Sec. IV. However, if the grazing angle falls within near the critical angle, spherical reflection coefficients[24] instead of plane wave ones are calculated in the forward model in order to incorporate the spherical wave effects, especially for the low frequency component.

Since there are numerous results on matched field inversion with vertical line arrays, a relatively good understanding of the sensitivity exists. However, less information is known on the time-domain inversions using a towed system and ship noises. In order to get better insights on the objective function and its sensitivity characteristics with respect to the geoacoustic parameters, we investigated the behavior of the objective function as a function of the selected parameter with other parameters fixed at their reference values. This sensitivity test is commonly carried out in practice in geoacoustic inversions. Although the sensitivity estimates using one parameter may show biased results due to parameter couplings,[25] it is considered meaningful to compare the sensitivity for our time-domain inversion with that of other matched field inversions.

For the sensitivity test, we assumed that the tow ship was a sound source and emitted both the random noise and a 320 Hz tonal signal. The environment was the same as Fig. 3. The noise generated by a tow ship propagated through the water column and one layered ocean sediment and was measured on 32 receivers of the HLA. The power spectrums of measured signals for all receivers are also shown in Fig. 3.

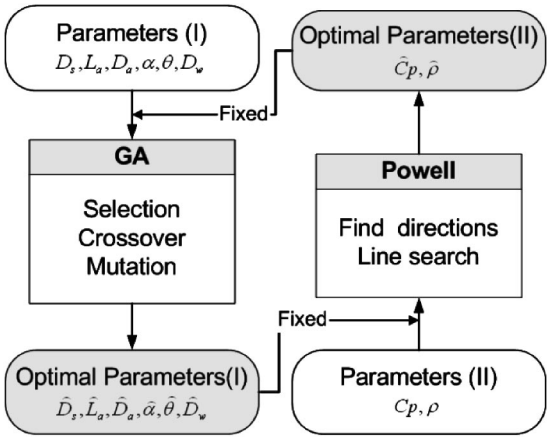

FIG. 6. Two-step optimization procedure.

Figure 4 shows the sensitivity curves of the parameters using 1 second data which correspond to 6000 time samples. The averaged time interval ΔT in Eq. (6) is chosen to be half the data length. The geometrical parameters such as the source position, the HLA configuration and the water depth show high sensitivities. The parameters of the layer and the sub-bottom show intermediate and low sensitivities, respectively. The sensitive parameters share a common characteristic in that they affect the travel times, i.e., phases, of the received signals. The least sensitive parameter which contributes to the wave amplitude is the density. The sound speed of the sub-bottom is also related with the amplitude in this simulation since a majority of the reflections from the sub-bottom interface occur before the total reflection range. In the simulated experimental setup, the covering angle of incidence with respect to vertical direction by the receivers ranges from 58° to 69°, but the critical angle of incidence is approximately 67°. The above results are mainly due to a nature of the matched impulse response filter. The physical meaning of the filtered output in Eq. (5) is the correlation between the measured signal and the simulated impulse response. The most influential factor in the correlation of the signals is the phase of each of the signal components. The differences in the phases result in a considerable reduction of correlation, but those of the amplitudes take little effect. Battle *et al.*[5] calculated the sensitivity of the sound speed of half space with respect to the distance between the source and HLA. According to them, the sensitivity showed a rapid increase as the source–receiver range approaches the critical range. After the critical range where the dependence of the reflection coefficient switches from amplitude to phase, the sensitivity saturated and then oscillated showing higher values than before the critical range. This implies that the parameter affecting the phase of the signal is very sensitive in the inversion.

IV. EXPERIMENT AND PARAMETRIZATION

The MAPEX 2000 ship noise experiment was conducted by the SACLANT Undersea Research Center near the island

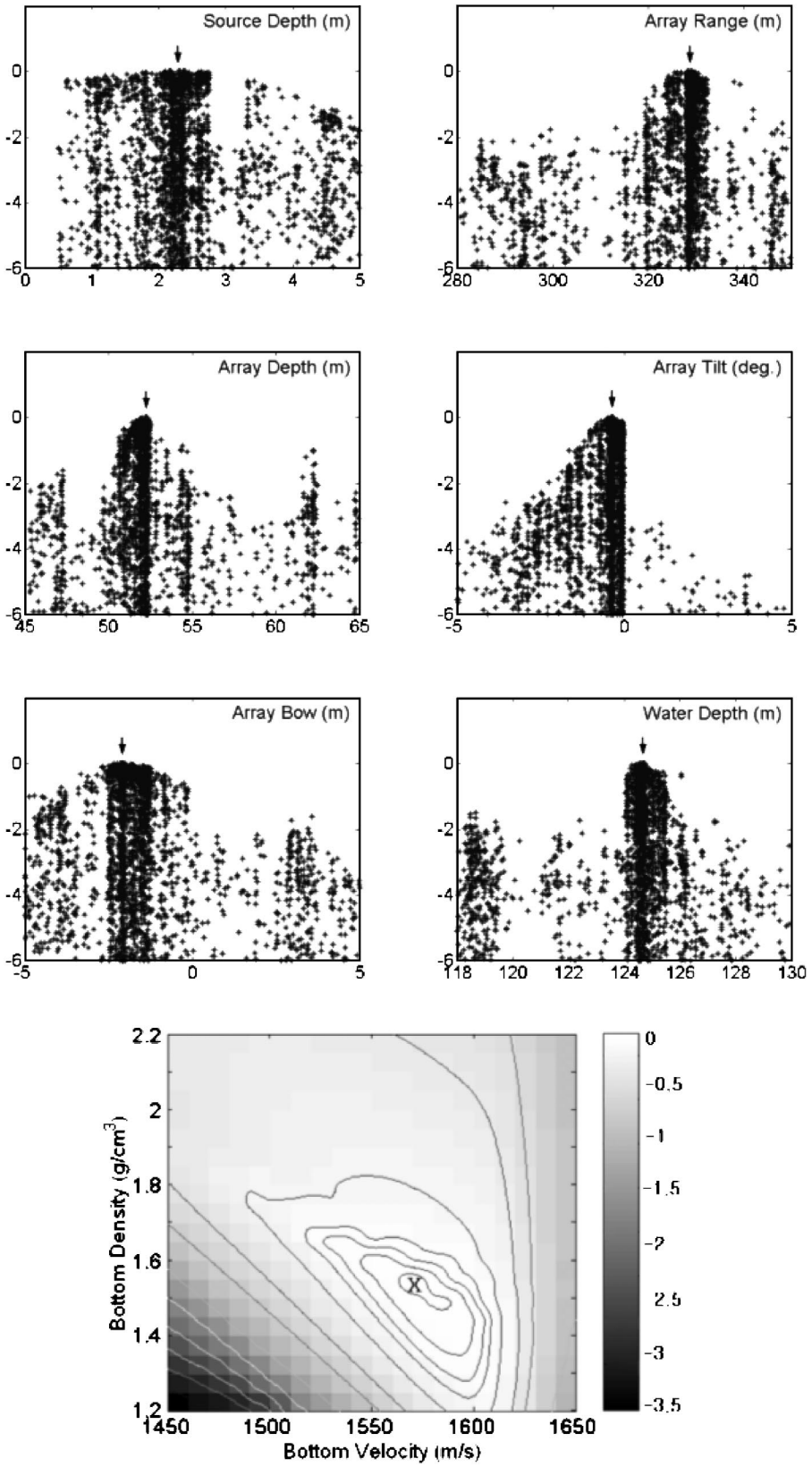

FIG. 7. Inversion results for data measured at 08:07:30 UTC (frame 100). The upper 6 figures are scatter plots of GA search and the lower two dimensional contour shows the objective function values which are re-evaluated based on the best parameters of GA and bottom parameters given in both x- and y-axes. Arrows and crosses represent the best solutions and all function values are given in dB normalized to the maximum value.

of Elba on November 29th. The data were received by a 254 m long HLA for 10 seconds every 30 seconds corresponding to data of 175 frames. The HLA was composed of 128 receivers with 2 m separations and was towed by the R/V *Alliance* along the track shown in Fig. 5.

From this figure, we can see that another R/V *Manning* was following the *Alliance* approximately 900 m behind along the same track from about frame 60 to frame 107. At frame 107, the *Alliance* started making a 45° turn, while the *Manning* proceeded on track as shown in Fig. 5. After frame

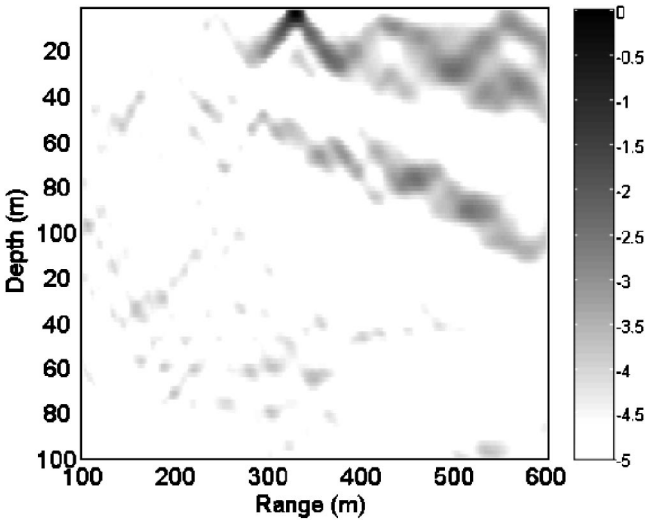

FIG. 8. Ambiguity surface of the source localization for the data measured at 08:07:30 UTC (frame 100) calculated using other inverted parameters except for the source location. The function values are given in dB normalized to the maximum value.

122, the *Manning* increased her speed and left the station. Since the distance between the *Alliance* and the nearest receivers to her was approximately 330 m, the horizontal range of the *Manning* from the tail of the array can be estimated to be about 320 m. Although the proximity of two ships may cause some interference, the *Manning* can still be utilized as a source of opportunity.

During the experiment, the depth-sounder recorded the bathymetry showing a slow growth from 116 m to 124 m for the entire track. The sound speed of the water column was kept almost constant at 1520 m/s according to expendable bathy-thermograph casts. The experimental sites have been studied for a long time and the bottom properties are well known. The bottom is comprised of a flat thin layer and a sub-bottom. The thin layer is composed of clay and clay–sand sediments and its thickness is approximately 2.5 m which is only a fraction of a wavelength at frequencies of a few hundred Hz. According to Gingras *et al.*,[26] the p-wave speed of the layer was estimated to increase linearly from 1505 m/s to 1556 m/s, which was *a posteriori* mean values based on the 40 observations. In each observation, however, the estimated upper and lower p-wave speeds of the layer showed high fluctuation. The estimated mean p-wave sound speed and density of the sub-bottom were 1578 m/s and 1.6 g/cm^3, respectively. Therefore, the thin layer is disregarded in the present inversion and the environmental model of the inversion is treated as range-independent infinite half space. The effect of the thin layer, which is assumed to be small and insensitive to wave propagation, will be included in the infinite half bottom properties in a depth-averaged manner.

Even though the towed HLA is devised to be neutrally buoyant in the water, it still remains to be susceptible to deformations in shape during operations. Therefore, the array shape needs to be included in the inversion parameters for reliable inversion results. Battle *et al.*[5] implemented the array shape deformation by defining the receiver depth as

$$z_i = \alpha\left(1 - \left(\frac{2x_i}{L}\right)^2\right) - x_i \sin\theta, \tag{8}$$

where x_i and z_i are the relative positions of the receiver with respect to the center of the array whose length is L. The inversion parameters α and θ in Eq. (8) represent the array bow and tilt, respectively. The same definition is adopted for our inversion. Consequently, a total of eight parameters will be inverted in subsequent inversions; source depth D_s, distance between the source and the nearest receiver L_a, depth of the array center D_a, array tilt θ, array bow α, water depth D_w, bottom sound speed Cp, and bottom density ρ. The attenuation of bottom will be excluded in the inversion due to its extremely low sensitivity.

V. INVERSION USING SOURCE OF OPPORTUNITY

There were two available sources, *Alliance* and *Manning*, used in this experiment. Among these two, the *Manning* data measured from frame 90 to frame 107 which corresponds to the track of thick line in Fig. 5 were considered in this paper. The data of each frame consisted of 10 second signals. Among the 128 receivers, we used every fourth receiver data (32 receivers) for the inversion. In addition, we divided each signal into 10 segments of 1 second long and inverted all of them.

Frequent traffic was reported near the experimental site and the data are possibly contaminated by other ships. Therefore, it was recommended to reduce the unwanted interferences using a wavenumber filter before inversion.[5] The wavenumber filter was implemented by a 2-D FFT for discrete time signals in a line array. It is noted when the wavenumber filtered data are used in the objective function (6), the simulated impulse response should also include only the corresponding rays. The wavenumber cutoff was set to include arrival angles falling within 50° of endfire to capture most of the expected multiple arrivals from the *Manning*.

The inversion was performed via an optimization process which searches the parameters to maximize the objective function in Eq. (6). Direct and surface reflected signals usually have large amplitudes. But they contain only the geometric information, such as the source and receiver positions, and thus are not useful for the inversion of bottom properties since they do not hit the bottom. If the geometry and bottom properties are inverted simultaneously, geometrical parameters will dominate over bottom parameters in the search process. In order to prevent such dominance in the optimization, the parameters should be inverted separately based on their sensitivities.

In geoacoustic inversion, global optimization methods such as the genetic algorithm and the simulated annealing are preferred due to their potential in finding a global optimum. However, they may have a drawback of slow convergence to the optimum. On the contrary, efficient local methods show quick and sure convergence to the optimum closest to the starting point, but it cannot guarantee to be the global optimum in the multi-modal function space. Presuming with reference to Fig. 4 that the multi-modality could be alleviated if we construct the objective function with only two parameters

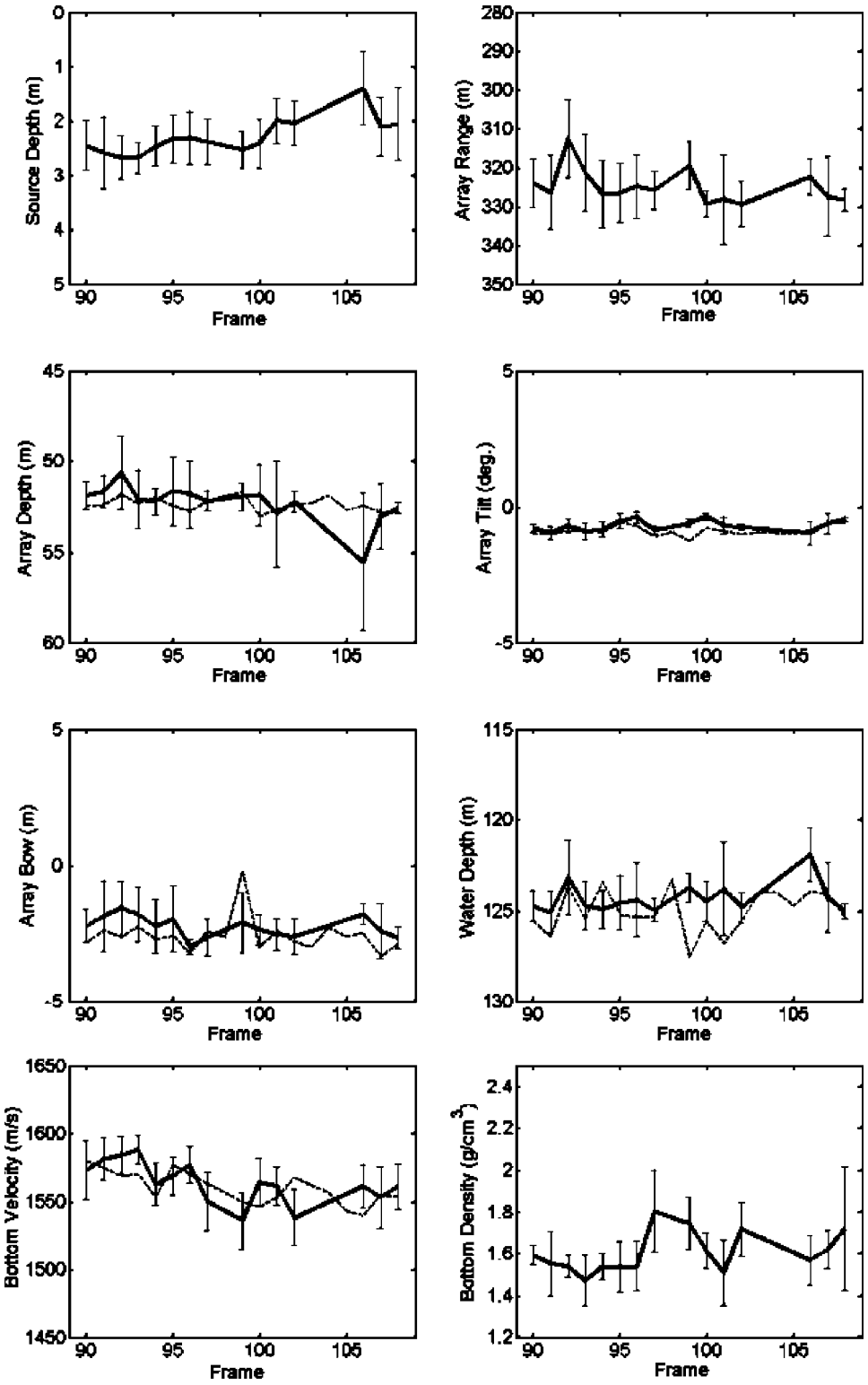

FIG. 9. The summary of inversion results which shows the mean and the standard deviation of 10 consecutive inversions of each frame by a thick line and error bars, respectively. The dashed lines represent reference values which were estimated by Battle *et al.* (Ref. 5) via a frequency domain matched field processing using tonal frequencies of 131.8, 262.9 and 306.9 Hz.

of bottom sound speed and bottom density, we took advantage of both the global and the local methods as follows.

At first, the genetic algorithm was applied to the sensitive parameters; the source depth, the array configurations and the water depth, and others fixed at certain values. After one generation of GA was constructed through the selection-crossover-mutation process, the remaining parameters were optimized using a local search method while already optimized parameters were kept at the best values among the population. And the GA search for the next generation was performed again with the insensitive parameters fixed at optimal values of the local search. The above two-step search process was repeated until a pre-determined number of generations. This optimization procedure is summarized in Fig. 6.

In the inversion, the GA searches were performed for 50 generations and each generation contained 60 populations. The crossover and mutation occurred with probabilities of

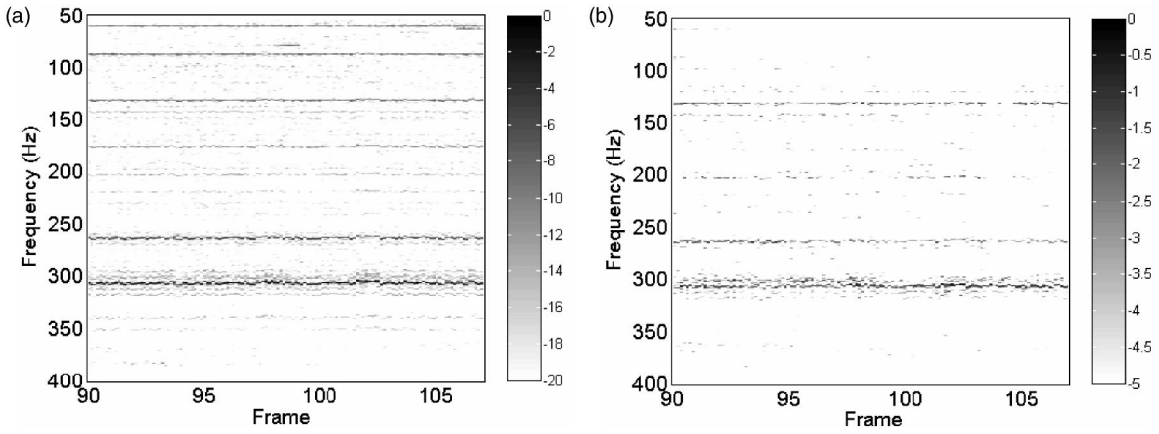

FIG. 10. A comparison of the spectrogram beamformed (a) and the Bartlett powers (b). The spectrogram was computed from beamformed time series in the *Manning* direction and the frequency dependent Bartlett powers were calculated with the inverted parameters of corresponding frame via time domain inversions. The function values are given in dB normalized to the maximum value.

0.9 and 0.05, respectively. Powell's method[27] was used as the local optimizer, since it does not need gradient information for finding its search direction.

A set of inversion results for a segment signal of frame 100 is presented in Fig. 7. Although one dimensional marginal *a posteriori* probability display of the results is a common practice,[14] we plotted all objective function values with respect to the corresponding parameter values visited during the GA search. By doing so, we could obtain information about the optimizer (GA) such as its behavior related to the parameter sensitivity and sampled parameter space.[10] For the insensitive bottom parameters, which are the main targets of the inversion, we re-evaluated the objective functions based on the best results of GA and showed them in a two dimensional contour plot in Fig. 7. In this figure, the arrows and the cross indicate the best solutions that were found during the inversion procedure. In the scatter plots of Fig. 7, all of the parameters of GA seem to have been resolved well. Besides, the two dimensional contour which shows the monomodality of the objective function space may be a result that supports that the local optimization is useful.

For an additional check of the validity for the inverted parameter values, we simply performed a back-propagation of the received signals from the array using these environmental parameter results of Fig. 7. The ambiguity surface in Fig. 8 shows a good focus of the back-propagated signals to the correct source position, considering that the draft of *Manning* and estimated range from the nearest receiver to her are 2.5 m and 320 m, respectively.

In Fig. 9, we summarize the inversion results of all frames by the statistical mean and standard deviation estimated from 10 multiple inversions at each frame. The ranges of the y-axis are the same with the search intervals in the optimization procedures. The standard deviations imply uncertainties of the inversion which may arise from the varying data SNR and environments during the experiment and/or from the inherent errors of the optimizer that may occur if the search space is vast.[28] However, the mean estimates seem to be consistent especially for geometric parameters irrespective of their uncertainties at each frame. The relatively high variability in the bottom densities seem to be due to its insensitivity to the wave propagation rather than to range dependencies, considering the experimental site has been known to be range independent. Besides, good agreements of our estimates with the reference values represented by the dashed lines in the figure are found. The reference values were estimated by Battle *et al.*[5] via a frequency domain matched field processing using tonal frequencies of 131.8, 262.9 and 306.9 Hz, which were identified as prominent peaks in the spectrogram of Fig. 10(a). The spectrogram was computed from beamformed time series in the *Manning* direction.

In this paper, we define the Bartlett power as a function of frequency f by

$$B_i(f) = \frac{\mathbf{w}^{\dagger}(f,\mathbf{m}_i)\mathbf{R}_i(f)\mathbf{w}(f,\mathbf{m}_i)}{\mathrm{tr}[\mathbf{R}_i(f)]\|\mathbf{w}(f,\mathbf{m}_i)\|^2}, \tag{9}$$

where $\mathbf{R}_i$ is the estimated cross spectral density matrix of the ith segmented signals and $\mathbf{w}(\mathbf{m}_i)$ represents the replica vector calculated with the inverted parameters of the corresponding segment. Figure 10(b) shows the calculated Bartlett power. Comparing it with the beamformed spectrogram of Fig. 10(a), we can see a similarity between them. From the frequency dependent behavior of the Bartlett power, it seems that a few frequencies played dominant roles in the inversion and they coincide with those used by Battle *et al.*, which naturally explains the agreements between the two different inversion results. Therefore, we can conclude that the proposed time domain inversion takes advantage of dominant frequencies of the source signature automatically.

VI. CONCLUSION

Predicting bottom properties is important for various acoustic applications in shallow waters due to the significance of the bottom interaction. In this paper we propose a feasible geoacoustic inversion method using a towed HLA and ship noises as a source of opportunity. Such a simple system may make immediate use of geoacoustic parameters as an input to various sonar operations possible.

The inversion scheme is summarized as follows. The objective function was defined using a matched impulse re-

sponse filter for the unknown source signal. The filtered output was implemented by back-propagating the received and time-reversed signals using a ray-based forward model. Then, a series of global and local searches was performed using GA and Powell's method, respectively, to find the optimum parameters.

The present method was applied to the experimental data of the MAPEX2000 noise experiment. The *Manning* data were inverted successively and their results showed good consistency for all parameters. The inverted parameters were compared with the reference values estimated via a frequency domain matched field processing using three dominant tonal frequencies and results showed good agreements. In addition, analyses of Bartlett power revealed that the proposed time domain inversion takes advantage of dominant frequencies of the source signature automatically.

ACKNOWLEDGEMENT

This work was supported by the Basic Research Program of KORDI/KRISO.

[1] N. R. Chapman and A. Tolstoy, ''Special issue: Benchmarking geoacoustical inversion methods,'' J. Comput. Acoust. **6**, 1–289 (1998).
[2] N. R. Chapman and M. Taroudakis, ''Special issue: Geoacoustic inversion in shallow water,'' J. Comput. Acoust. **8**, 259–388 (2000).
[3] W. A. Kuperman, M. F. Werby, K. E. Gilbert, and G. J. Tango, ''Beam forming on bottom-interacting tow-ship noise,'' IEEE J. Ocean. Eng. **10**, 290–298 (1985).
[4] M. Siderius, P. Nielsen, and P. Gerstoft, ''Range-dependent seabed characterization by inversion of acoustic data from a towed receiver array,'' J. Acoust. Soc. Am. **112**, 1523–1535 (2002).
[5] D. Battle, P. Gerstoft, W. A. Kuperman, W. S. Hodgkiss, and M. Siderius, ''Geoacoustic inversion of tow-ship noise using matched-field processing,'' IEEE J. Ocean. Eng. **28**, 454–467 (2003).
[6] C. Park, W. Seong, P. Gerstoft, and M. Siderius, ''Time domain geoacoustic inversion of high-frequency chirp signal from a simple towed system,'' IEEE J. Ocean. Eng. **28**, 468–478 (2003).
[7] N. R. Chapman, R. M. Dizaji, and R. L. Kirlin, ''Geoacoustic inversioln using broad band ship noise,'' *Proceedings of the 5Pth ECUA*, Lyon, 2000, pp. 787–792.
[8] D. P. Knobles and R. A. Koch, ''A time series analysis of sound propagation in a strongly mutipath shallow water environment with an adiabatic normal mode approach,'' IEEE J. Ocean. Eng. **21**, 290–298 (1985).
[9] J.-P. Hermand, ''Broad-band geoacoustic inversion in shallow water from waveguide impulse response measurements on a single hydrophone: theory and experimental results,'' IEEE J. Ocean. Eng. **24**, 41–66 (1999).
[10] L. Jaschke and N. R. Chapman, ''Matched field inversion of broadband data using the freeze bath method,'' J. Acoust. Soc. Am. **106**, 1838–1851 (1999).
[11] C. W. Holland and J. Osler, ''High-resolution geoacoustic inversion in shallow water: a joint time- and frequency-domain technique,'' J. Acoust. Soc. Am. **107**, 1263–1279 (2000).
[12] P. Pignot and N. R. Chapman, ''Tomographic inversion of geoacoustic properties in a range-dependent shallow-water environment,'' J. Acoust. Soc. Am. **110**, 1338–1348 (2001).
[13] N. R. Chapman, J. Desert, A. Agarwal, Y. Stephan, and X. Demoulin, ''Estimation of seabed models by inversion of broadband acoustic data,'' *Proceedings of the 6Pth ECUA*, Gdansk, 2002, pp. 477–481.
[14] P. Gerstoft, ''Inversion of seismoacoustic data using genetic algorithms and *a posteriori* probability distribution,'' J. Acoust. Soc. Am. **95**, 770–782 (1994).
[15] S. E. Dosso, M. L. Yeremey, J. M. Ozard, and N. R. Chapman, ''Estimation of ocean-bottom properties by matched-field inversion of acoustic field data,'' IEEE J. Ocean. Eng. **18**, 232–239 (1993).
[16] P. Gerstoft, ''Inversion of acoustic data using a combination of genetic algorithm and the Gauss-Newton approach,'' J. Acoust. Soc. Am. **97**, 2181–2190 (1995).
[17] M. R. Fallat and S. E. Dosso, ''Geoacoustic inversion via local, global, and hybrid algorithms,'' J. Acoust. Soc. Am. **105**, 3219–3230 (1999).
[18] T. B. Nielsen, ''An iterative implementation of rotated coordinates for inverse problems,'' J. Acoust. Soc. Am. **113**, 2574–2586 (2003).
[19] A. Parvulescu and C. S. Clay, ''Reproducibility of signal transmission in the ocean,'' Radio Electron. Eng. **29**, 223–228 (1965).
[20] C. S. Clay, ''Optimum time domain signal transmission and source location in a waveguide,'' J. Acoust. Soc. Am. **81**, 660–664 (1987).
[21] R. K. Brienzo and W. S. Hodgkiss, ''Broadband matched-field processing,'' J. Acoust. Soc. Am. **94**, 2821–2831 (1993).
[22] D. R. Jackson and D. R. Dowling, ''Phase conjugation in underwater acoustics,'' J. Acoust. Soc. Am. **89**, 171–181 (1991).
[23] D. R. Dowling, ''Acoustic pulse compression using passive phase-conjugate processing,'' J. Acoust. Soc. Am. **95**, 1450–1458 (1994).
[24] L. M. Brekhovskikh, *Waves in Layered Media*, 2nd ed. (Academic, New York, 1980).
[25] S. E. Dosso, ''Quantifying uncertainty in geoacoustic inversion. I. A fast Gibbs sampler approach,'' J. Acoust. Soc. Am. **111**, 129–142 (2002).
[26] D. F. Gingras and P. Gerstoft, ''Inversion for geometric and geoacoustic parameters in shallow water: Experimental results,'' J. Acoust. Soc. Am. **97**, 3589–3598 (1995).
[27] W. H. Press, S. A. Teukolsky, W. T. Vetterling, and B. P. Flannery, *Numerical Recipes in C*, 2nd ed. (Cambridge University Press, Cambridge, 1992).
[28] M. Snellen, D. G. Simons, M. Siderius, J. Sellschopp, and P. L. Nielsen, ''An evaluation of the accuracy of shallow water matched field inversion results,'' J. Acoust. Soc. Am. **109**, 514–527 (2001).